Biogeosciences Discuss., https://doi.org/10.5194/bg-2017-269
Manuscript under review for journal Biogeosciences
Discussion started: 29 June 2017

Biogeosciences Discussions
Open Access
EGU

Physiological and biochemical responses of *Emiliania huxleyi* to ocean acidification and warming are modulated by UV radiation

Shanying Tong[1], David A. Hutchins[2], Kunshan Gao[1]

[1]State Key Laboratory of Marine Environmental Science, Xiamen University, Xiamen, China

[2]Department of Biological Sciences, University of Southern California, Los Angeles, California, USA

Correspondence to: Kunshan Gao (ksgao@xmu.edu.cn)

Biogeosciences Discuss., https://doi.org/10.5194/bg-2017-269
Manuscript under review for journal Biogeosciences
Discussion started: 29 June 2017

Abstract

Marine phytoplankton such as bloom-forming, calcite-producing coccolithophores, are naturally exposed to solar UV radiation (UVR, 280-400 nm) in the ocean's upper mixed layers. Nevertheless, effects of increasing CO_2-induced ocean acidification and warming have rarely been investigated in the presence of UVR. We examined calcification and photosynthetic carbon fixation performance in the most cosmopolitan coccolithophorid, *Emiliania huxleyi*, grown under high (1000 µatm, HC; pH_T: 7.70) and low (400 µatm, LC; pH_T: 8.02) CO_2 levels, at 15 ℃ (LT), 20 ℃ (MT) and 24 ℃ (HT) with or without UVR. The HC treatment didn't affect photosynthetic carbon fixation at 15 ℃, but significantly enhanced it with increasing temperature. Exposure to UVR inhibited photosynthesis, with higher inhibition by UVA (320-395 nm) than UVB (295-320 nm), except in the HC and 24 ℃-grown cells, in which UVB caused more inhibition than UVA. Reduced thickness of the coccolith layer in the HC-grown cells appeared to be responsible for the UV-induced inhibition, and an increased repair rate of UVA-derived damage in the HCHT-grown cells could be responsible for lowered UVA-induced inhibition. While calcification was reduced with the elevated CO_2 concentration, exposure to UVB or UVA affected it differentially, with the former inhibiting and the latter enhancing it. UVA-induced stimulation of calcification was higher in the HC-grown cells at 15 and 20 ℃, whereas at 24 ℃, observed enhancement was not significant. The calcification to photosynthesis ratio (Cal/Pho ratio) was lower in the HC treatment, and increasing temperature also lowered the value. However, at 20 and 24 ℃, exposures to UVR significantly increased the Cal/Pho ratio, especially in HC-grown cells, by up to 100%. This implies that UVR can counteract the negative effects of the 'greenhouse' treatment on the Cal/Pho ratio, and so may be a key stressor when considering the

impacts of future greenhouse conditions on *E.huxleyi*.

Key words: *Emiliania huxleyi*, ocean acidification, temperature, UV radiation, photosynthesis, calcification

1 Introduction

Coccolithophores are a group of calcifying unicellular phytoplankton within the Prymnesiophyceae (Paasche, 2002). They are an ecologically and biogeochemically prominent marine phytoplankton functional group, and contribute to carbon dioxide sinks and sources by performing both photosynthesis and calcification, respectively (Raitsos et al., 2006; Raven and Crawfurd, 2012). Although the ballasting of photosynthetic products by coccoliths helps to efficiently transport carbon from the photic zone, the calcification process is a net source of CO_2 to the environment (Gattuso et al., 1996; Rost and Riebesell, 2004). Therefore, the ratio of photosynthesis to calcification determines their net contribution to carbon dioxide uptake or release. Consequently, investigating changes in these two processes under varying environmental conditions is a key to our understanding of their biogeochemical roles under ocean global change. Calcification and photosynthesis of coccolithophores are influenced by many factors, including nutrients, light availability, and CO_2, as well as temperature and ultraviolet radiation (UVR) (Feng et al., 2008; Riebesell et al., 2017; Tong et al., 2016) .

Rising atmospheric CO_2 concentration due to human activities causes greenhouse warming of the atmosphere and ocean, and the dissolution of this anthropogenic CO_2 into the surface ocean reduces the pH of seawater in a process known as ocean acidification (OA). Ongoing OA has been predicted to decrease pH by 0.40 units in

pelagic waters (Gattuso et al., 2015) and by 0.45 (Cai et al., 2011) units in coastal waters (Cai et al., 2011) by the end of this century under the business-as-usual CO_2 emissions scenario. On the other hand, increased atmospheric CO_2, along with other greenhouse gases, will warm the Earth's surface by 2.5-6.4 ℃ by the year 2100 (Alexiadis, 2007), while the surface ocean temperature is projected to rise by 2-3 ℃ (Stocker et al., 2014). Ocean warming will enhance water column stratification and lead to shallower upper mixed layers, thus exposing phytoplankton cells within these layers to higher integrated levels of photosynthetically active and ultraviolet radiation (UVR) (Courtial et al., 2017). Stratification will also lead to reduced upward transport and lower availability of nutrients.

All these ocean global changes may have individual and/or interactive effects on the physiology of marine primary producers (Gao et al., 2012; Hutchins and Fu, 2017) . OA usually decreases calcification of *E. huxleyi*, although corresponding pCO_2 increases can enhance photosynthesis or growth at the same time (Riebesell et al., 2017; Riebesell et al., 2000). Under nutrient replete conditions, increased light levels appear to counteract the negative impacts of OA on calcification on *E. huxleyi* (Jin et al., 2017). The calcified coccoliths are thought to play roles in protections against grazing pressure, viral and bacterial attack (Monteiro et al., 2016), and can also help protect cells from UV radiation (Gao et al., 2009) . Early experiments on *E .huxleyi* strain BT-6 showed that cells had a complete covering of coccoliths at 12.5 to 23 ℃, but at 26.5 ℃, 30% of the cells had an incomplete covering (Paasche, 1968). Similarly, Langer et al. (2009) saw increased malformed coccoliths in *E. huxleyi* RCC 1238 at 25 ℃ compared to those grown at 20 and 10 ℃ . A recent study showed that

increased temperature aggravates the impacts of OA on *E. huxleyi* morphology (Milner et al., 2016).

Increasing levels of PAR or temperature and changes in UVR and nutrient availability may interact with each other to cause additive, antagonistic or synergistic effects on coccolithophores. Nevertheless, most previous studies have been carried out under PAR only, without UVR or fluctuating solar radiation being considered. However, UVR cannot be ignored when examining the effects of environmental changes on marine phytoplankton that are found in the upper half of the euphotic zone, since UV irradiance can penetrate as deep as 80 m in pelagic waters (Tedetti et al., 2007). Excessive solar UV-B and UV-A can damage DNA and interfere with many cellular biochemical processes (Häder et al., 2014). On the other hand, moderate levels of UVA can enhance photosynthetic carbon fixation of phytoplankton assemblages (Gao et al., 2007; Helbling et al., 2003). As for UVR effects on coccolithophore calcification, recent studies demonstrated that the outer coccoliths of *E. huxleyi* can effectively shield the cells from a certain percentage of UVR radiation (Xu et al., 2016). Nevertheless, the transmitted energy still causes significant inhibition of calcification, as well as photosynthesis (Gao et al., 2009). Exposure of *E. huxleyi* to solar UV radiation decreased its growth rate, but increased its production of coccoliths per cell (Guan and Gao, 2009).

Since exposure to solar UV radiation can influence cytoplasmic redox activities (Wu et al., 2010), and inhibit or enhance physiological performances at different levels of UVR, we hypothesized that effects of OA and warming on coccolithophores would be

different with and without the presence of UVR. To test our hypothesis, in this study we examined the responses of *E. huxleyi* photosynthesis and calcification to OA with or without UVR at three temperature levels.

2. Materials and methods

2.1 Experimental setup

Experiments used *Emiliania huxleyi* strain PML B92/11, originally isolated from the field station of the University of Bergen, Norway (Raunefjorden; 60 °18'N, 05 °15'E). To first test interactions between OA and temperature, thermal reaction curves were obtained by growing the cultures at 15, 20, 22, 24 and 27 ℃ in artificial seawater pre-equilibrated with elevated (1000 µatm, HC) or ambient (400 µatm, LC) atmospheric CO_2 concentrations. Triplicate experimental cultures were maintained without aeration under PAR (cool-white fluorescent lamps) of 190 µmol $m^{-2}s^{-1}$ with a 12/12 light/dark cycle. The culture medium was enriched with 100 µmol l^{-1} nitrate and 10 µmol l^{-1} orthophosphate, and vitamins and trace metals were added according to the Aquil recipe (Sunda et al., 2005). The maximum cell concentration in all treatments was maintained below 5×10^4 cells ml^{-1} in order to maintain stable carbonate chemistry (pH variation <0.04). After the cells were grown in each treatment for about 10 generations, the growth rates were determined. Then the thermal reaction norms were plotted for HC- and LC-grown cells according to the equation:

$$f(T)=ae^{bT}\left[1-\left(\frac{T-z}{w/2}\right)^2\right] \quad (1),$$

where w is the temperature niche width, z is the midpoint of the growth curve, and b and a jointly determine the overall steepness, height, and skewness of the curves (Norberg, 2004; Thomas et al., 2012). The optimum temperature for growth (T_{opt}) was

estimated from the fitted curve by numerical optimization.

Based on T_{opt} from the thermal curve, 15, 20 and 24 ℃ were selected to grow the cells for another 10 generations. The rationale for choosing these temperatures is that 15 and 20 ℃ are below and close to the optimal growth temperature, while 24 ℃ is above it. To investigate how the cells responded to these three different levels of temperature and two pCO_2 levels in the presence of transient UV irradiance exposures such as might be encountered by cells in a dynamic mixed layer, they were then exposed to the different radiation treatments for three hours before photosynthesis and calcification parameters were measured (section 2.2.3).

2.2 Measurements and analysis

2.2.1 Growth rates

The specific growth rates (μ) were determined from cell counts performed with a Z2 Coulter Counter (Beckman, Buckinghamshire, UK), calculated using the equation: $\mu = (\ln C_1 - \ln C_0)/(t_1 - t_0)$, where t_0 and t_1 were the times of inoculation and sampling, $t_1 - t_0$ was the interval between inoculation and sampling, and C_0 and C_1 were the cell concentrations at time t_0 and t_1.

2.2.2 POC, PON and PIC analysis and estimation of inner coccosphere volume

After cells were cultured at 15, 20, and 24 ℃ for another 10 generations, duplicate samples (200 mL) taken in the middle of the light period were filtered onto 25 mm precombusted (450 ℃ for 6h) Whatman GF/F filters and stored at -20 ℃. For analysis, one of the duplicate filters for each treatment was fumed over HCl for 12h to remove inorganic carbon and then dried overnight at 60 ℃; the other filters were dried overnight at 60 ℃ directly. All the filters were then packed in tin cups and

analyzed on a Perkin Elmer Series II CHNS/O Analyzer 2400. PIC was determined by the difference between TPC (total particulate carbon) and POC. The production rates of POC or PIC were calculated as P = cellular POC or PIC content (pg $cell^{-1}$) ×specific growth rate μ (d^{-1})

The inner coccosphere (protoplast) volume (V_{cell}) were calculated according to:

$$\frac{POC[pg]}{cell} = a \times V_{cell}^{b} \quad (2)$$

Where a (0.216 in this case) and b (0.939 in this case) are constants which vary depending on the investigated species (Menden-Deuer and Lessard, 2000).

2.2.3 Radiation treatment and determination of calcification and photosynthetic rates

Right before the elemental samples were taken, the cells acclimated to each temperature and pCO_2 level were dispensed into 90 ml quartz tubes (volume 100 ml) and inoculated with 5μCi (0.185 MBq) of labeled sodium bicarbonate (ICN Radiochemicals). The quartz tubes were then exposed to a solar simulator with PAR, UVA and UVB irradiance levels of 42 W m^{-2} (190 μmol $m^{-2}s^{-1}$), 13.5 W m^{-2}, and 0.81 W m^{-2}, respectively. The radiation intensity was measured using a three channel irradiation apparatus (PAM2100, Solar Light). The PAR used was equivalent to the mean light level in the upper mixed layer (UML) based on time series station (19 °N, 118.5 °E) measurements in the South China Sea (Chen et al., 2006). The ratios of both UVA and UVB to PAR emitted by the solar simulator were about 30% higher than those of the sunlight reaching the sea surface. The following three radiation treatments were realized: PAR+UVA+UVB (PAB), quartz tubes covered with 295 nm cut-off film (Ultraphan, Digefra), so that the cells were exposed to irradiances above 295 nm; PAR+UVA (PA), covered with 320 nm cutoff film (Montagefolie, Folex), with the cells exposed to irradiances above 320 nm; and PAR (P), covered with 395

nm cutoff film (Ultraphan UV Opak, Digefra), so that the cells received irradiances above 395 nm. The temperatures were controlled with a cooling circulator (CAP-3000, Rikakikai, Japan). The exposure duration lasted for 3h, and each treatment had 3 replicates for the incubations. This short exposure period under the solar simulator can mimic mixing of cells to the surface or the reappearance of sunlight after cloudiness, both of which occur frequently in nature.

The collected samples from each treatment were immediately filtered onto Whatman GF/F filters (25mm), rinsed with unlabeled medium, and then put in 20 ml scintillation vials. One filter from each tube was fumed over HCl overnight to remove the coccolith coverage, and then dried at 45 ℃ for 4 h to estimate the photosynthetic carbon fixation rate, while other filters were dried directly to estimate the total carbon fixation rate. 3.5 ml scintillation cocktail (Perkin Elmer) were added to the vials, and all the filters were counted using a liquid scintillation counter (LS6500 Multi-Purpose Scintillation Counter, Beckman Counter, USA). The rate of calcification was determined as the difference between total and photosynthetic carbon fixation rate. The inhibition of calcification and photosynthesis due to UVA, UVR, or UVB was calculated as:

$Inh_{UVA} = (R_P - R_{PA})/(R_P) \times 100\%$

$Inh_{UVR} = (R_P - R_{PAB})/(R_P) \times 100\%$

$Inh_{UVB} = (R_{PA} - R_{PAB})/(R_P) \times 100\% = Inh_{UVR} - Inh_{UVA}$

Where R_P, R_{PA}, and R_{PAB} represented the rate of calcification or photosynthesis under PAR, PAR+UVA and PAR+UVA+UVB respectively.

2.2.4 Estimation of carbonate chemistry

The pH of the seawater was measured with a pH meter (Benchtop pH510, Oakton) that was calibrated with standard NBS (National Bureau of Standards) buffer. The

CO_2 concentration of the aeration was monitored with a CO_2 meter (Vaisala, GM70) with variations < 4%. The cell concentrations of all cultures were maintained below 5×10^4 cells ml^{-1} to make sure pH variations were <0.04 units. Other seawater carbonate system parameters were calculated with the CO2SYS software using the known parameters of pCO_2, salinity, pH, temperature and nutrient concentrations (Lewis et al., 1998). The carbonic acid dissociation equilibrium constants K_1 and K_2 were determined according to Roy et al. (1993) and that for boric acid was from Dickson (1990).

2.2.5 Data Analysis

Before parametric tests were performed, data were tested for homogeneity of variance and normality. Two-way or three-way analysis of variance (ANOVA) were used to establish differences among the treatments. The two sample paired t-test was also used to determine significant differences between temperature, CO_2 or UV treatments. Significance levels were set at $p<0.05$.

3 Results

3.1 Thermal reaction norms

The growth temperature curve (growth thermal norms) obtained for *E. huxleyi* (Fig. 1) exhibited different shapes in the LC and the HC-grown cells. The LC cultures showed an asymmetric pattern that is common to many algal species, in which the growth rate increased with rise of temperature to reach a maximum of 1.3 d^{-1} at 22.2 ℃ and then declined sharply at temperatures above this optimal point. At 20 and 24 ℃, growth rate was <10% lower compared to 22.2 ℃, so 20 and 24 ℃ were still within the optimal growth temperature range for LC-grown *E. huxleyi*. The HC-grown cells showed a relatively symmetric thermal norm, with an optimal growth temperature at 20.6 ℃, 1.6 ℃ lower than that of the LC-grown ones. Thus the growth rate at 20 ℃

was near maximal, while the value at 24 ℃ decreased by nearly 20% compared to the maximal growth rate. The net effect of these trends was that growth rate of the LC-grown cells was significantly ($p<0.05$) higher than that of the HC-grown cells at 22 and 24 ℃ (Fig. 1).

3.2 Growth rate

During the 10 generations of growth at two CO_2 levels and three temperatures prior to the UV exposure, the growth rate was lowest at 15 ℃ and was further reduced by 17.4% in HC-grown cells compared to LC-grown ones ($p<0.05$, Fig. 2). At 20 ℃, there was no difference in growth rates between HC- and LC-grown cells ($p>0.05$). At 24 ℃, growth rate didn't change in LC-grown cells ($p>0.05$), but decreased in HC-grown ones compared to that at 20 ℃, and thus the value was 17.5 % lower in HC-grown cells compared to LC-grown ones at 24 ℃ ($p>0.05$).

3.3 Cellular PIC and POC quotas, production rates and inner coccosphere volumes

The two CO_2 treatments had no effect on cellular POC content at 15 ℃ and 20 ℃. However, at 24 ℃, the HC treatment significantly increased cellular POC by 18.4% compared to the LC treatment ($p<0.01$, Fig. 3a), yielding the highest value among the treatments. Cellular PIC content was reduced with increased CO_2 concentration in the 15, 20, and 24 ℃ treatments by 35.8% ($p<0.05$, Fig. 3b), 62.6% ($p<0.05$) and 17.1% ($p<0.01$), respectively. In LC-grown cells, cellular PIC was significantly affected by temperature, being the highest at 15 ℃, and was decreased by 34.2% ($p<0.01$) at 20 ℃ and 18.9% ($p<0.01$) at 24 ℃. In HC-grown cells, cellular PIC was 45.2 % ($p<0.01$) and 41.7% ($p<0.01$) lower at 20 ℃, compared to at 15 and 24 ℃, respectively. The production rate of POC ranged from 6.8 to 13.2 pg $cell^{-1}d^{-1}$ among different treatments (Fig. 3c). At 15 ℃, the HC treatment reduced POC production

rate by 26.6% ($p<0.05$), and the values were 42% ($p<0.01$) and 30% ($p<0.01$) lower in HC- and LC-grown cells respectively compared to those at 20 ℃. No significant differences were observed between different CO_2 treatments at 20 ℃ and 24 ℃ ($p>0.05$), and the temperature rising from 20 to 24 ℃ also had no significant effect on POC production rate both in HC- and LC-grown cells ($p>0.05$). The HC treatment lowered the PIC production rate by 42.3% ($p<0.01$, Fig. 3d), 37.3% ($p<0.01$), and 29.9% ($p<0.01$) at 15, 20, and 24 ℃ respectively. A 5 ℃ temperature decrease from 20 ℃ had no significant effect on PIC production rate both in LC- and HC-cultures ($p>0.05$). However, a 4 ℃ increase from 20 to 24 ℃ enhanced the PIC production rate by 41.9% ($p<0.05$) and 27.4% ($p<0.05$) in HC- and LC-grown cells respectively.

The pattern of inner coccosphere volume among different treatments was similar to that of cellular POC (Fig. 3e), with a significantly higher value in HC-cultures than LC-ones at 24 ℃ ($p<0.01$), while no difference existed between different CO_2 treatments at the other temperature levels ($p>0.05$).

The PIC to POC ratio (PIC/POC) had the lowest value at 20 ℃ in the HC treatment (Fig. 3f), and the highest value at 15 ℃ in the LC treatment. Either reduced or elevated temperature from 20 ℃ increased the PIC/POC ratio in both HC- and LC-cultures ($p<0.05$), although the extent varied.

3.4 Cellular PON content

Cellular PON had the same trends between the HC and LC treatments at 15 and 20 ℃ ($p>0.05$, Fig. 4). Similar to cellular POC, at 24 ℃ cellular PON was 29.6% higher in HC-grown cells compared to LC-grown ones ($p<0.01$).

3.5 Responses of calcification and photosynthetic carbon fixation to UV radiation

After 3 h of exposure under the solar simulator, significant interactive effects between temperature and irradiance ($p<0.01$), temperature and pCO_2 ($p<0.01$), and irradiance

and pCO_2 (p=0.042) were observed on photosynthetic carbon fixation. There were no differences in photosynthetic carbon fixation rates between HC- and LC-cultures at 15 ℃ under the PAR alone treatment (p>0.05, Fig. 5a), while the values were marginally (p=0.064, Fig. 5b) and significantly higher (p=0.026, Fig. 5c) in HC-grown cells compared to LC-grown ones at 20 and 24 ℃. At 15 ℃, the photosynthetic rate was lowered by the same extent under the PA and PAB treatments compared to the PAR treatment in HC conditions (p<0.01), while the presence of UVA or UVR (UVA+UVB) had no significant effects on photosynthetic rate under LC conditions (p>0.05). At 20 ℃, the values were reduced by 33.4% (p<0.05) and 19.9% (p=0.05) in HC- and LC-grown cells under the PA treatment compared to the PAR alone treatment. The PAB treatment didn't further lower the photosynthetic rates compared to the PA treatment in either the HC- or LC-cultures (p>0.05). At the highest temperature of 24 ℃, the photosynthetic rate was 22.6% (p<0.01) and 34.8% (p<0.01) lower under the PA treatment compared to the PAR alone treatment in HC- and LC-grown cells respectively. The values were further decreased by 35.7% (p<0.01) in HC-grown cells, but weren't affected in LC-grown ones in the PAB treatment (p>0.05).

Calcification rates were significantly lower in HC-grown cells compared to LC-grown ones under the PAR alone treatment at all temperature levels (p<0.01, Fig. 5 d, e, f). The PA treatment significantly increased the calcification rate in HC-grown cells relative to the PAR alone treatment, regardless of temperature levels (p<0.05). However, there were no significant differences in calcification rates between PA and PAR treatments in LC-grown cells (p>0.05). Under the PAB treatment, the presence of UVB led to a reduced calcification rate compared to the PA treatment at 15 ℃ (p<0.01), but had no significant effect at 20 and 24 ℃ (p>0.05) in either HC- or

LC-grown cells. There were significant interactions between temperature and irradiance on calcification rate ($p=0.018$).

Calcification to photosynthesis ratio (Cal/Pho ratio) values were significantly higher under PA than in the PAR alone treatment ($p<0.05$, Fig. 5 g, h, i), regardless of the CO_2 concentrations and temperature levels. The Cal/Pho ratio was lower at 15 ℃ under PAB compared to the PA treatment in both HC- ($p<0.01$) and LC-grown cells ($p<0.05$), while there were no significant differences between those irradiance treatments at 20 ℃ and 24 ℃ ($p>0.05$). Except in the PA treatment at 15 ℃, the Cal/Pho ratio was significantly lower in HC-grown cells compared to LC-grown ones under all the other conditions, with the greatest reduction of 44.3% at 24 ℃. There were significant interactions among all three variables for the Cal/Pho ratio ($p<0.01$).

3.6 UVR-induced inhibition of photosynthetic carbon fixation and calcification

There were significant interactions among the three variables for inhibition of photosynthesis relative to the PAR alone treatment ($p<0.01$, Fig. 6 1,2,3). UVA-induced inhibition of photosynthesis was higher in HC-grown cells compared to LC-grown ones at 15 and 20 ℃ ($p<0.05$), while this pattern was reversed at 24 ℃. UVB-induced inhibition of photosynthesis was much higher in HC-grown cells than in LC-grown ones at 24 ℃ ($p=0.04$), but was not significantly different between HC and LC treatments at the other two temperature levels ($p>0.05$). As a whole, the HC treatment induced a higher inhibition by UVR (UVA+UVB) than the LC treatment, although the differences were not statistically significant ($p>0.1$). In most cases, UVA-induced inhibition of photosynthesis was significantly higher than inhibition induced by UVB, except in the HC treatment at 24 ℃, where UVA inhibition was lower than that induced by UVB ($p<0.05$), and in the LC treatment at 20 ℃, where there was no difference for UVA- and UVB-induced inhibition.

UVA stimulated calcification rates by 31.7% and 18.9% in HC-grown cells at 15 and 20 ℃ respectively (depicted in Figs. 6 d and e as negative inhibition rates). The effect of UVA on calcification rate was not statistically significant in LC-grown cells ($p>0.05$). At 24 ℃, the stimulation of calcification rate by UVA in HC-grown cells compared to LC-grown ones was not significant ($p>0.05$, Fig.6 f). UVB inhibited calcification rates in all treatments, with the greatest inhibition being in HC-cultures at 15 ℃. Due to the opposite effects of UVA and UVB on calcification rate, the total inhibition induced by UVR was not significant at 20 and 24 ℃ ($p>0.05$). At 15 ℃, the UVR-induced inhibition was marginally higher in HC-grown cells than LC-grown ones ($p=0.052$).

When the inhibition of the Cal/Pho ratio was assessed, the UVB-induced inhibition was much higher in the HC treatment at 15 ℃ than in all other conditions (Fig. 6g, h, i). The UVA stimulated Cal/Pho ratio was much higher in HC- grown cells compared to LC-grown ones at 15 ℃, while there was no significant difference between the HC and LC treatments at 20 and 24 ℃. Both types of UVR together had no net effect on the Cal/Pho ratio at 15 ℃, but significantly stimulated the Cal/Pho value at 20 and 24 ℃ under both CO_2 conditions ($p<0.05$).

4 Discussion

Our results demonstrated that both photosynthesis and calcification were inhibited by UVB. In contrast, UVA was more inhibitory for photosynthesis than UVB, while it had a positive effect on calcification. The degree to which UVA and UVB affected the performance of photosynthesis and calcification varied depending on CO_2 concentrations and temperature levels. Of the three temperature levels used, 15 ℃ was much lower than optimal growth temperature for both HC- and LC- grown cells. For LC cultures, the growth rate was the same at 20 and 24 ℃, and those two

370 temperatures were in the optimal range for cells growth. While 20 ℃ was very close
371 to the optimal temperature for HC-grown cells, the growth rate at 24 ℃ was
372 significantly reduced, suggesting the cells growth at this temperature may be already
373 thermally inhibited. The different growth state among the three temperature levels,
374 particularly that between HC- and LC-grown cells at the highest temperature,
375 potentially affected the photosynthetic and calcification responses to UV radiation.
376 In this study, the inhibition of photosynthesis by UVA, UVB and their combination
377 appeared to increase with temperature. On the contrary, previous studies conducted on
378 other phytoplankton species such as diatoms suggested that increasing temperature
379 could reduce UV-induced inhibition of photosynthesis, as the activities of repair
380 associated enzymes are temperature dependent (Helbling et al., 2011; Li et al., 2012).
381 These differing trends between the present and previous studies may be attributed to
382 either changes in the thickness of the coccolith layer surrounding the cells, or to the
383 temperature range used. The coccoliths of *E. huxleyi* can provide a protective role
384 against UVR either by strongly scattering light, or by physically shading intracellular
385 organelles (Voss et al., 1998; Xu et al., 2016). In our results, the cellular PIC at 20 ℃
386 was only half of that at 15 ℃. Since cellular PIC is an indicator of the amount of
387 coccoliths on the exterior of the cell, this suggests that the cells grown at 20 ℃ had a
388 substantially thinner coccolith layer and so received much more UV radiation, leading
389 to increased photosynthetic damage compared to cells grown at 15 ℃. At 24 ℃, the
390 thermal reaction curves suggested that this temperature level was already close to the
391 upper tolerance limit for growth in *E. huxleyi* PML B92/11, with HC-grown cells
392 suffering more thermal stress. At this temperature, though the thickness of coccolith
393 layer was equal to that at 15 ℃, biochemical aspects of UVR defense and /or repair
394 mechanisms may be under thermal stress (Sobrino and Neale, 2007).

At 15 and 20 ℃ the inhibition of photosynthesis was mainly caused by UVA, and the values were significantly higher in HC-grown cells compared to LC-grown ones, due to a thinner coccolith layer on cells in acidified seawater (Gao et al., 2009). In contrast, at 24 ℃ the HC treatment alleviated the UVA-induced inhibition but greatly enhanced inhibition by UVB. The underlying mechanism may be protein-mediated defense/repair processes. This is supported by the fact that cellular PON was increased by the HC treatment only at 24 ℃. Cellular PON content can reflect the defense and repair ability of cells against UVR (Litchman et al., 2002; Sobrino et al., 2008). The widely observed UV protection strategy in marine organisms is the production of nitrogen-rich UVR absorbing compounds known as mycosporine-like amino acids (MAAs) (Banaszaka and Lesser, 2009). Phytoplankton use several mechanisms to repair UV-induced damage, many of which involve N-requiring enzymes and/or protein cofactors (Litchman et al., 2002). Korbee et al. (2010) reported that UVA could stimulate algae N metabolism (nitrate transport and reductase activity). In contrast, UVB was found to damage cell membranes and negatively affect nitrogen incorporation mechanisms, leading to a decrease in cellular PON content (Sobrino et al., 2004). Subsequently, such a lack of nitrogen would inhibit essential protein turnover. In our study at 24 ℃, UVA and HC might act synergistically to maintain higher cellular PON content and support the synthesis of MAAs and UV-repair proteins, thereby partially counteracting the UV-induced damage. Although MAAs were not examined here, recent studies revealed that these substances can be effectively synthesized by *E. huxleyi* exposed to UV radiation (Xing et al., 2014) and cellular MAA contents were significantly higher under high CO_2 conditions (Gao and Zheng, 2010). As mentioned above, at 24 ℃ HC-grown cells were already thermally inhibited, which may add the detrimental effect of UVB on

nitrogen assimilation and lead to much higher inhibition of photosynthesis by UVB in high CO_2, warmer conditions.

When assessing the effect of UV radiation on calcification, we found that UVA stimulated calcification rate of *E. huxleyi* PML B92/11, while UVB inhibited it. In earlier studies, Gao et al. (2009) reported that both UVA and UVB negatively affected calcification of *E. huxleyi* CS-369. One possibility is that this discrepancy between our studies can be attributed to strain-specific responses. On the other hand, the different irradiances used by the two studies could be involved, as the light intensity used by Gao et al. (2009) was over twice as high as the one we used. Like our study, Xu and Gao (2015) also observed that moderate levels of UVR increased PIC production rates.

Here, we speculate on the possible underlying mechanisms for UVA-stimulated calcification. First, it has been documented in some algae that the reduced levels of UVA energy can be transferred through the electron transport chain of PS II in the same way as PAR (Xu and Gao, 2010b). This however could not be the reason for the UVA-stimulated calcification of *E .huxleyi*, since the photosynthetic process was significantly inhibited by UVA at the same time. Second, it has been demonstrated that both CO_2 and bicarbonate in seawater can supply carbon to photosynthesis, while only bicarbonate is used by *E. huxleyi* to make its coccoliths (Kottmeier et al., 2016; Paasche, 2002) . It has been shown that UVA alone could drive bicarbonate utilization (Xu and Gao, 2010a). In our case, the stimulation of calcification by UVA may be attributed to a more available inorganic carbon source (bicarbonate). The UVA-induced stimulation of calcification was higher in the HC treatment at 15 and 20 ℃, due to more transmitted UVA with a reduced thickness of the coccolith layer in HC-grown cells. At 24 ℃, however, no difference in the UVA effect was found

between the HC and LC treatments, likely because the inner coccosphere volume of the HC-grown cells was significantly enlarged, leading to an extended pathlength of UVA through cells.

Given that the responses of coccolithophore strains to environmental change can be different depending on that strain's temperature optimum (Sett et al., 2014), the temperatures we chose in this study were below, close or above optimum for *E. huxleyi* growth based on its thermal tolerance curves. The temperatures we used also have important ecological significance. *E. huxleyi* blooms are most extensive in the Subarctic North Atlantic from summer to autumn, the region where our *E. huxleyi* strain was isolated (Brown, 1995). A large proportion of annual coccolithophore production can occur in a single seasonal bloom event, with a significant impact on regional ecology and global biogeochemical cycles (Lampert et al., 2002).

The lower temperature of 15 ℃ that we used was around the mean summer surface water temperature in the region where *E. huxleyi* PML B92/11 was isolated (Fielding, 2013). 20 ℃ on the other hand represents a future warmer condition, with 24 ℃ being likely similar to the upper limit of temperatures that will be experienced by this strain due to temperature fluctuations in the future. In the present study, we found that UV radiation could interact with both temperature and CO_2 concentration to alter their effects on photosynthesis and calcification, thus changing Cal/Pho ratios. Under the PAR alone treatment, Cal/Pho ratios were lower in HC cultures compared to LC ones regardless of temperature levels, and the values were also further reduced with increasing temperatures. In the presence of UVR (UVA+UVB), Cal/Pho ratios were significantly increased at 20 and 24 ℃, and this response that was enhanced in HC-grown cells. In contrast, UVR had no effect on Cal/Pho ratios at 15 ℃. This implies that the presence of UVR could counteract and partially compensate for the

reduced C/P ratios caused by ocean warming and acidification, with potentially important effects on the ocean carbon cycle.

In previous studies, most indoor laboratory experiments neglected the effects of UV radiation due to the common use of UV-free light sources or UV-opaque vessels. Our results demonstrated that UV radiation could greatly influence the combined effects of future CO_2 enrichment and sea surface warming on the physiological performance of *E. huxleyi*. Thus, the impacts UV radiation should be considered in order to build more realistic predictions of future biological and biogeochemical processes in a high CO_2 ocean.

Author contributions: Shanying Tong and Kunshan Gao designed the study. The experiment was performed by S.T. S.T. analysed the data and wrote the manuscript. David Hutchins and K.G. contributed to the revision and approved the final version of the manuscript.

Competing interests: the authors declare that they have no conflict of interest.

Acknowledgements: This study was supported by National Natural Science Foundation (41430967; U1606404), the national key research programs (2016YFA0601400) and State Oceanic Administration.

References

Alexiadis, A.: Global warming and human activity: A model for studying the potential instability of the carbon dioxide/temperature feedback mechanism, Ecol. Modell., 203, 243-256, 2007.

Banaszaka, A. T. and Lesser, M. P.: Effects of solar ultraviolet radiation on coral reef organisms, Photochemical & Photobiological Sciences, 8, 1276-1294, 2009.

Brown, C. W.: Global distribution of Coccolithophore blooms, The Future Of Oceanography, 8, 59-60, 1995.

Cai, W.-J., Hu, X., Huang, W.-J., Murrell, M. C., Lehrter, J. C., Lohrenz, S. E., Chou, W.-C., Zhai, W., Hollibaugh, J. T., and Wang, Y.: Acidification of subsurface coastal waters enhanced by eutrophication, Nature Geoscience, 4, 766-770, 2011.

Chen, C.-C., Shiah, F.-K., Chung, S.-W., and Liu, K.-K.: Winter phytoplankton blooms in the shallow mixed layer of the South China Sea enhanced by upwelling, J. Mar. Syst., 59, 97-110, 2006.

Courtial, L., Roberty, S. e., Shick, J. M., Houlbre`que, F., and Ferrier-Page`s, C.: Interactive effects of ultraviolet radiation and thermal stress on two reef-building corals, Limnol. Oceanogr., doi: 10.1002/lno.10481, 2017. 2017.

Dickson, A. G.: Standard potential of the reaction: AgCl (s)+ 12H2 (g)= Ag (s)+ HCl (aq), and and the standard acidity constant of the ion HSO 4− in synthetic sea water from 273.15 to 318.15 K, The Journal of Chemical Thermodynamics, 22, 113-127, 1990.

Feng, Y., Warner, M. E., Zhang, Y., Sun, J., Fu, F.-X., M.Rose, J., and Hutchins, D. A.: Interactive effects of increased pCO_2, temperature and irradiance on the marine coccolithophore *Emiliania huxleyi* (Prymnesiophyceae), Eur. J. Phycol., 43, 87-98, 2008.

Fielding, S. R.: *Emiliania huxleyi* specific growth rate dependence on temperature, Limnol. Oceanogr., 58, 663-666, 2013.

Gao, K., Helbling, E. W., Häder, D.-P., and Hutchins, D. A.: Responses of marine primary producers to interactions between ocean acidification, solar radiation, and warming, Mar. Ecol.: Prog. Ser., 470, 167-189, 2012.

Gao, K., Ruan, Z., Villafan, V. E., Gattuso, J.-P., and Helbling, E. W.: Ocean acidification exacerbates the effect of UV radiation on the calcifying phytoplankter *Emiliania huxleyi*, Limnol. Oceanogr., 54, 1855-1862, 2009.

Gao, K., Wu, Y., Li, G., Wu, H., e, V. E. V., and Helbling, E. W.: Solar UV Radiation Drives CO_2 Fixation in Marine Phytoplankton: A Double-Edged Sword, Plant Physiol., 144, 54-59, 2007.

Gao, K. and Zheng, Y.: Combined effects of ocean acidification and solar UV radiation on photosynthesis, growth, pigmentation and calcification of the coralline alga *Corallina sessilis*
(Rhodophyta), Global Change Biol., 16, 2388-2398, 2010.

Gattuso, J.-P., Magnan, A., Billé, R., Cheung, W. W. L., Howes, E. L., Joos, F., Allemand, D., Bopp, L., Cooley, S. R., Eakin, C. M., Hoegh-Guldberg, O., Kelly, R. P., Pörtner, H.-O., Rogers, A. D., Baxter, J. M., Laffoley, D., Osborn, D., Rankovic, A., Rochette, J., Sumaila, U. R., Treyer, S., and Turley, C.: Contrasting futures for ocean and society from different anthropogenic CO_2 emissions scenarios, Science, 349, 2015.

Gattuso, J.-P., Pichon, M., and Frankignoulle, M.: Biological control of air-sea CO_2 fluxes: effect of photosynthetic and calcifying marine organisms and ecosystems, Oceanographic Literature Review, 7, 663-664, 1996.

Guan, W. and Gao, K.: Impacts of UV radiation on photosynthesis and growth of the

542 coccolithophore *Emiliania huxleyi* (Haptophyceae), Environ. Exp. Bot., 67, 502-508,
543 2009.
544 Häder, D.-P., Williamson, C. E., Wängberg, S.-Å., Rautio, M., Rose, K. C., Gao, K.,
545 Helbling, E. W., Sinhah, R. P., and Worrest, R.: Effects of UV radiation on aquatic
546 ecosystems and nteractions with other environmental factors, Photochemical &
547 Photobiological Sciences, doi: 10.1039/c4pp90035a, 2014. 2014.
548 Helbling, E. W., Buma, A. G. J., Boelen, P., Strate, H. J. v. d., Giordanino, M. V. F.,
549 and Villafañe, V. E.: Increase in Rubisco activity and gene expression due to elevated
550 temperature partially counteracts ultraviolet radiation-induced photoinhibition in the
551 marine diatom *Thalassiosira weissflogii*, Limnol. Oceanogr., 56, 1330-1342, 2011.
552 Helbling, E. W., Gao, K., Gonçalves, R. J., Wu, H., and Villafañe, V. E.: Utilization of
553 solar UV radiation by coastal phytoplankton assemblages off SE China when exposed
554 to fast mixing, Mar. Ecol. Prog. Ser., 259, 59-66, 2003.
555 Hutchins, D. A. and Fu, F.: Microorganisms and ocean global change, Nature
556 microbiology, 2, 2017.
557 Jin, P., Ding, J., Xing, T., Riebesell, U., and Gao, K.: High levels of solar radiation
558 offset impacts of ocean acidification on calcifying and non-calcifying strains of
559 *Emiliania huxleyi*, Mar. Ecol.: Prog. Ser., 568, 47-58, 2017.
560 Korbee, N., Mata, M. T., and Figueroa, F. l. L.: Photoprotection mechanisms against
561 ultraviolet radiation in Heterocapsa sp. (Dinophyceae) are influenced by nitrogen
562 availability: Mycosporine-like amino acids vs. xanthophyll cycle, Limnol. Oceanogr.,
563 55, 899-908, 2010.
564 Kottmeier, D. M., Rokitta, S. D., and Rost, B.: Acidification, not carbonation, is the
565 major regulator of carbon fluxes in the coccolithophore *Emiliania huxleyi*, New
566 Phytol., 2016. 2016.
567 Lampert, L., Queguiner, B., Labasque, T., Pichon, A., and Lebreton, N.: Spatial
568 variability of phytoplankton composition and biomass on the eastern continental shelf
569 of the Bay of Biscay (north-east Atlantic Ocean). Evidence for a bloom of *Emiliania*
570 *huxleyi* (Prymnesiophyceae) in spring 1998, Cont. Shelf Res., 22, 1225-1247, 2002.
571 Langer, G., Nehrke, G., Probert, I., Ly, J., and Ziveri, P.: Strain-specific responses of
572 *Emiliania huxleyi* to changing seawater carbonate chemistry, Biogeosciences, 6,
573 2637-2646, 2009.
574 Lewis, E., Wallace, D., and Allison, L. J.: Program developed for CO_2 system
575 calculations, Carbon Dioxide Information Analysis Center, managed by Lockheed
576 Martin Energy Research Corporation for the US Department of Energy Tennessee,
577 1998.
578 Li, Y., Gao, K., ˜ne, V. E. V., and Helbling, E. W.: Ocean acidification mediates
579 photosynthetic response to UV radiation and temperature increase in the diatom
580 *Phaeodactylum tricornutum*, Biogeosciences, 9, 3931-3942, 2012.
581 Litchman, E., Neale, P. J., and Banaszak, A. T.: Increased sensitivity to ultraviolet
582 radiation in nitrogen-limited dinoflagellates: Photoprotection and repair, Limnol.
583 Oceanogr., 47, 86-94, 2002.
584 Menden-Deuer, S. and Lessard, E. J.: Carbon to volume relationships for
585 dinoflagellates, diatoms, and other protist plankton, Limnol. Oceanogr., 45, 569-579,

2000.
Milner, S., Langer, G., Grelaud, M., and Ziveri, P.: Ocean warming modulates the effects of acidification on *Emiliania huxleyi* calcification and sinking, Limnology and Oceanography, 61, 1322-1336, 2016.
Monteiro, F. M., Bach, L. T., Brownlee, C., Bown, P., Rickaby, R. E., Poulton, A. J., Tyrrell, T., Beaufort, L., Dutkiewicz, S., and Gibbs, S.: Why marine phytoplankton calcify, Science Advances, 2, e1501822, 2016.
Norberg, J.: Biodiversity and ecosystem functioning: A complex adaptive systems approach, Limnol. Oceanogr., 49, 1269-1277, 2004.
Paasche, E.: The effect of temperature, light intensity, and photoperiod on coccolith formation, Limnol. Oceanogr., 13, 178-181, 1968.
Paasche, E.: A review of the coccolithophorid *Emiliania huxleyi* (Prymnesiophyceae), with particular reference to growth, coccolith formation, and calcification-photosynthesis interactions, Phycologia, 40, 503-529, 2002.
Raitsos, D. E., Lavender, S. J., Pradhan, Y., Tyrrell, T., Reid, P. C., and Edwards, M.: Coccolithophore bloom size variation in response to the regional environment of the subarctic North Atlantic, Limnol. Oceanogr., 51, 2122-2130, 2006.
Raven, J. A. and Crawfurd, K.: Environmental controls on coccolithophore calcification, Mar. Ecol.: Prog. Ser., 470, 137-166, 2012.
Riebesell, U., Bach, L. T., Bellerby, R. G. J., Monsalve, J. R. B., Boxhammer, T., Czerny, J., Larsen, A., Ludwig, A., and Schulz, K. G.: Competitive fitness of a predominant pelagic calcifier impaired by ocean acidification, Nature Geoscience, 10, 19-24, 2017.
Riebesell, U., Zondervan, I., Rost, B. r., Tortell, P. D., Zeebe, R. E., and Morel, F. o. M. M.: Reduced calcification of marine plankton in response to increased atmospheric CO2, Nature, 407, 364-367, 2000.
Rost, B. and Riebesell, U.: Coccolithophores and the biological pump: responses to environmental changes. In: Coccolithophores, Springer, 2004.
Roy, R. N., Roy, L. N., Vogel, K. M., Porter-Moore, C., Pearson, T., Good, C. E., Millero, F. J., and Campbell, D. M.: The dissociation constants of carbonic acid in seawater at salinities 5 to 45 and temperatures 0 to 45 C, Marine Chemistry, 44, 249-267, 1993.
Sett, S., Bach, L. T., Schulz, K. G., Koch-Klavsen, S., Lebrato, M., and Riebesell, U.: Temperature Modulates Coccolithophorid Sensitivity of Growth, Photosynthesis and Calcification to Increasing Seawater pCO2, Plos noe, 9, 1-9, 2014.
Sobrino, C., Montero, O., and Lubián, L. M.: UV-B radiation increases cell permeability and damages nitrogen incorporation mechanisms in *Nannochloropsis gaditana*, Aquatic Sciences, 66, 421-429, 2004.
Sobrino, C. and Neale, P. J.: Short-term and long-term effects of temperature on photosynthesis in the diatom *Thalassiosira Pseudonana* under UVR exposures, J. Phycol., 43, 426-436, 2007.
Sobrino, C., Ward, M. L., and Neale, P. J.: Acclimation to elevated carbon dioxide and ultraviolet radiation in the diatom *Thalassiosira pseudonana*: Effects on growth, photosynthesis, and spectral sensitivity of photoinhibition, Limnol. Oceanogr., 53,

494-505, 2008.
Stocker, T., Qin, D., Plattner, G.-K., Tignor, M., Allen, S. K., Boschung, J., Nauels, A., Xia, Y., Bex, V., and Midgley, P. M.: Climate change 2013: The physical science basis, Cambridge University Press Cambridge, UK, and New York, 2014.
Sunda, W. G., Price, N. M., and Morel, F. M.: Trace metal ion buffers and their use in culture studies, Algal culturing techniques, 4, 35-63, 2005.
Tedetti, M., Sempéré, R., Vasilkov, A., Charriere, B., Nérini, D., Miller, W. L., Kawamura, K., and Raimbault, P.: High penetration of ultraviolet radiation in the south east Pacific waters, Geophysical Research Letters, 34, 2007.
Thomas, M. K., Kremer, C. T., Klausmeier, C. A., and Litchman, E.: A Global Pattern of Thermal Adaptation in Marine Phytoplankton, Science, 338, 1085-1088, 2012.
Tong, S., Hutchins, D. A., Fu, F., and Gao, K.: Effects of varying growth irradiance and nitrogen sources on calcification and physiological performance of the coccolithophore *Gephyrocapsa oceanica* grown under nitrogen limitation, Limnol. Oceanogr., 61, 2234-2242, 2016.
Voss, K. J., Balch, W. M., and Kilpatrick, K. A.: Scattering and attenuation properties of *Emiliania Huxleyi* cells and their detached coccoliths, Limnol. Oceanogr., 43, 870-876, 1998.
Wu, Y., Gao, K., Li, G., and Helbling, E. W.: Seasonal Impacts of Solar UV Radiation on Photosynthesis of Phytoplankton Assemblages in the Coastal Waters of the South China Sea, Photochem. Photobiol., 86, 586-592, 2010.
Xing, T., Gao, K., and Beardall, J.: Response of Growth and Photosynthesis of *Emiliania huxleyi* to Visible and UV Irradiances under Different Light Regimes, Photochem. Photobiol., 2014. 2014.
Xu, J., Bach, L. T., Schulz, K. G., Zhao, W., and Gao, K.: The role of coccoliths in protecting *Emiliania huxleyi* against stressful light and UV radiation, Biogeosciences, 13, 4637-4643, 2016.
Xu, J. and Gao, K.: Use of UV-A Energy for Photosynthesis in the Red Macroalga *Gracilaria lemaneiformis*, Photochem. Photobiol., 86, 580-585, 2010a.
Xu, J. and Gao, K.: UV-A enhanced growth and UV-B induced positive effects in the recovery of photochemical yield in *Gracilaria lemaneiformis* (Rhodophyta), Plant Biotechnol. J. B, 100, 117-122, 2010b.
Xu, K. and Gao, K.: Solar UV Irradiances Modulate Effects of Ocean Acidification on the Coccolithophorid *Emiliania huxleyi*, Photochem. Photobiol., 91, 92-101, 2015.

Biogeosciences Discuss., https://doi.org/10.5194/bg-2017-269
Manuscript under review for journal Biogeosciences
Discussion started: 29 June 2017

669 Table 1. Mean values of the seawater carbonate system parameters under HC (1000
670 μatm) and LC (400 μatm) at 15, 20 and 24 °C. The cell concentrations of all cultures
671 were maintained below 5×10^4 cells ml^{-1} and pH variations were <0.04 units. The
672 superscripts represent significant difference between HC and LC ($p<0.05$).

	Treatment	pH_{NBS}	DIC ($\mu mol\ kg^{-1}$)	pCO_2 (μatm)	HCO_3^- ($\mu mol\ kg^{-1}$)	CO_3^{2-} ($\mu mol\ kg^{-1}$)	Total alkalinity ($\mu mol\ kg^{-1}$)
15 ℃	HC	7.80 ±0.02[a]	2147.2 ±105.7[a]	1000 ±40[a]	2037.5 ±98.6[a]	72.4 ±7[a]	2228.5 ±114.4[a]
	LC	8.13 ±0.01[b]	1919.2 ±27.2[b]	400 ±40[b]	1768.1 ±23.6[b]	136.2 ±3.6[b]	2122.8 ±31.7[a]
20 ℃	HC	7.82 ±0.01[a]	2153.2 ±57.3[a]	1000 ±40[a]	2031.5 ±52.8[a]	89.74 ±4.5[a]	2262.7 ±62.9[a]
	LC	8.16 ±0.01[b]	1961.8 ±25.7[b]	400 ±40[b]	1777.8 ±21.8[b]	170.13 ±3.9[b]	2214.38 ±30.4[a]
25 ℃	HC	7.84 ±0.01[a]	2057.2 ±28.1[a]	1000 ±40[a]	2174.8 ±26.2[a]	106.3 ±2.5[a]	2310.3 ±31.2[a]
	LC	8.18 ±0.01[b]	1854.6 ±46.5[b]	400 ±40[b]	1999.8 ±38.4[b]	203.1 ±8.2[b]	2297.2 ±56.4[a]

673
674
675
676
677
678
679
680
681
682
683

Biogeosciences Discuss., https://doi.org/10.5194/bg-2017-269
Manuscript under review for journal Biogeosciences
Discussion started: 29 June 2017

Table 2. The optimal temperature for growth (T_{opt}) and the maximum growth rate (μ_{max}) at T_{opt} of *E.huxleyi* grown in 400 µatm (LC) and 1000 µatm (HC) CO_2 concentrations. T_{opt} and μ_{max} as estimated from the fitted curves in Fig. 1 by numerical optimization.

	T_{opt} (℃)	μ_{max} (µ)
HC	20.58	1.22
LC	22.15	1.31

Biogeosciences Discuss., https://doi.org/10.5194/bg-2017-269
Manuscript under review for journal Biogeosciences
Discussion started: 29 June 2017

Table 3. Three-way ANOVA analyses of interactive effects among pCO_2 (CO_2), temperature (T), and irradiance (I, including P, PA and PAB) on photosynthetic carbon fixation rates, calcification rates and Cal/Pho ratios respectively. Also shown are three-way ANOVA analyses of interactive effects among CO_2 (CO_2), temperature (T) and irradiance (I, including UVA, UVB and UVR) on the inhibition of photosynthesis, calcification and Cal/Pho ratios respectively. "*" and "**" represent significance levels at $p<0.05$ and 0.01 respectively.

	T×I *p* (df, F)	T×CO_2 *p* (df, F)	I×CO_2 *p* (df, F)	T×I×CO_2 *p* (df, F)
Pho rate	<0.01**	<0.01**	0.042*	0.055
	(4, 7.220)	(2, 11.505)	(2, 3.453)	(4, 2.560)
Cal rate	0.018*	0.541	0.465	0.483
	(4, 3.432)	(2, 0.625)	(2, 0.783)	(4, 0.885)
Cal/Pho ratio	<0.01**	0.03*	0.632	0.002**
	(4, 8.253)	(2, 3.874)	(2, 0.464)	(4, 5.155)
Inh of Pho rate	0.231	0.381	0.565	<0.01**
	(4, 1.473)	(2, 0.991)	(2, 0.580)	(4, 8.546)
Inh of cal rate	0.01**	0.24	<0.01**	<0.01**
	(4, 3.928)	(2, 1.484)	(2, 8.881)	(4, 6.610)
Inh of Cal/Pho ratio	0.021*	0.108	0.127	<0.01**
	(4, 3.331)	(2, 2.365)	(2, 2.186)	(4, 6.727)

719 Fig. 1 Thermal reaction norms of *E. huxleyi* grown in 400 µatm (LC) and 1000 µatm
720 (HC) CO_2 concentrations. Corresponding R^2=0.996 (LC) and 0.999 (HC), respectively.
721 The values are the means and the error bars are standard deviations for triplicate
722 cultures at each treatment.
723 Fig. 2 Specific growth rate of *E. huxleyi* grown in 400 µatm (LC) and 1000 µatm (HC)
724 CO_2 concentrations at 15 ℃, 20 ℃ and 24 ℃ respectively. The different letters above
725 the bars indicate significant differences among the treatments ($p<0.05$). The values are
726 the means and the error bars are standard deviations for triplicate cultures at each
727 treatment.
728 Fig. 3 Cellular POC (a), cellular PIC (b), POC production rate (c), PIC production rate
729 (d), inner coccosphere volume (e) and PIC/POC ratio (f) of *E. huxleyi* grown in 400
730 µatm (LC) and 1000 µatm (HC) CO_2 concentrations at 15 ℃, 20 ℃ and 24 ℃
731 respectively. The different letters above the bars indicate significant differences
732 among the treatments ($p<0.05$). The values are the means and the error bars are
733 standard deviations for triplicate cultures at each treatment.
734 Fig. 4 Cellular PON content of *E. huxleyi* grown in 400 µatm (LC) and 1000 µatm
735 (HC) CO_2 concentrations at 15 ℃, 20 ℃ and 24 ℃ respectively. The different letters
736 above the bars indicate significant differences among the treatments ($p<0.05$). The
737 values are the means and the error bars are standard deviations for triplicate cultures
738 at each treatment.
739 Fig. 5 Photosynthetic carbon fixation rates (a, b, c), calcification rates (d, e, f) and
740 Cal/Pho ratios (g, h, i) of *E. huxleyi* in HC- and LC-grown cells exposed to P

(irradiances above 395 nm), PA (irradiances above 320 nm) and PAB (irradiances above 295 nm) at 15, 20 and 25 ℃. Lines above the histogram bars indicate significant differences between HC and LC treatment, and different letters indicate significant differences among the radiation treatments within the HC or LC-grown cells within each panel.

Fig. 6 Inhibition of photosynthetic carbon fixation rates (a, b, c), calcification rates (d, e, f) and Cal/Pho ratios (g, h, i) of *E. huxleyi* in HC- and LC-grown cells due to UVA, UVB and UVR at 15, 20 and 25 ℃. Negative inhibition values indicate stimulation. Lines above the histogram bars indicate significant differences between HC and LC treatment, and different letters indicate significant differences among the radiation treatments within the HC or LC-grown cells within each panel.

Biogeosciences Discuss., https://doi.org/10.5194/bg-2017-269
Manuscript under review for journal Biogeosciences
Discussion started: 29 June 2017

763 Fig. 1

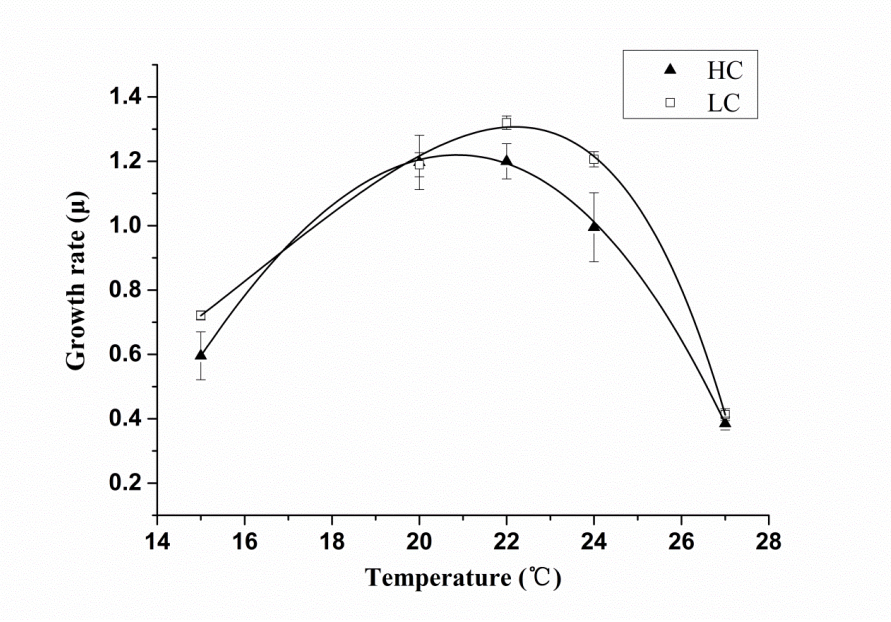

764

765

766

767

768

769

770

771

772

773

774

775

776

Biogeosciences Discuss., https://doi.org/10.5194/bg-2017-269
Manuscript under review for journal Biogeosciences
Discussion started: 29 June 2017

777 Fig. 2

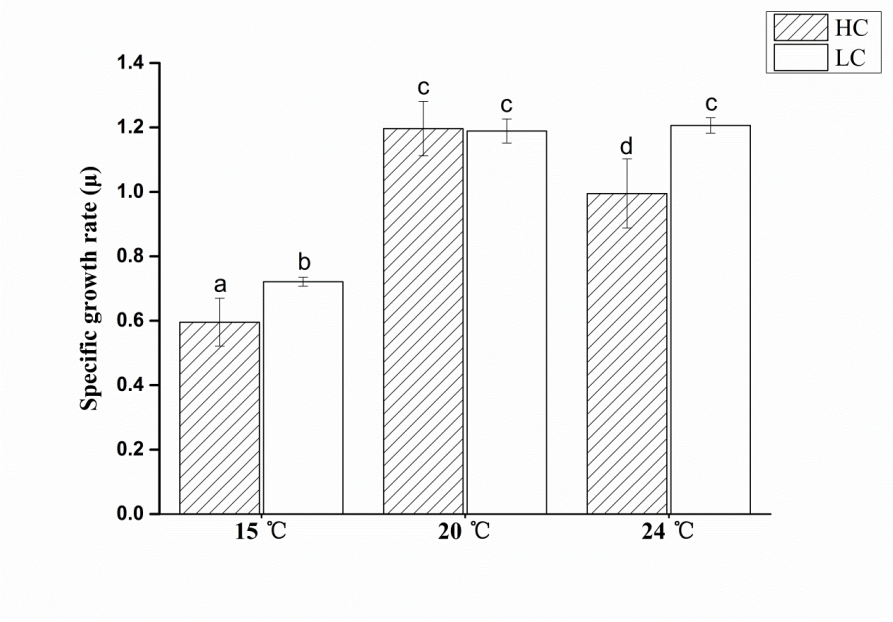

778

779

780

781

782

783

784

785

786

787

788

789

790

Biogeosciences Discuss., https://doi.org/10.5194/bg-2017-269
Manuscript under review for journal Biogeosciences
Discussion started: 29 June 2017

791 Fig 3

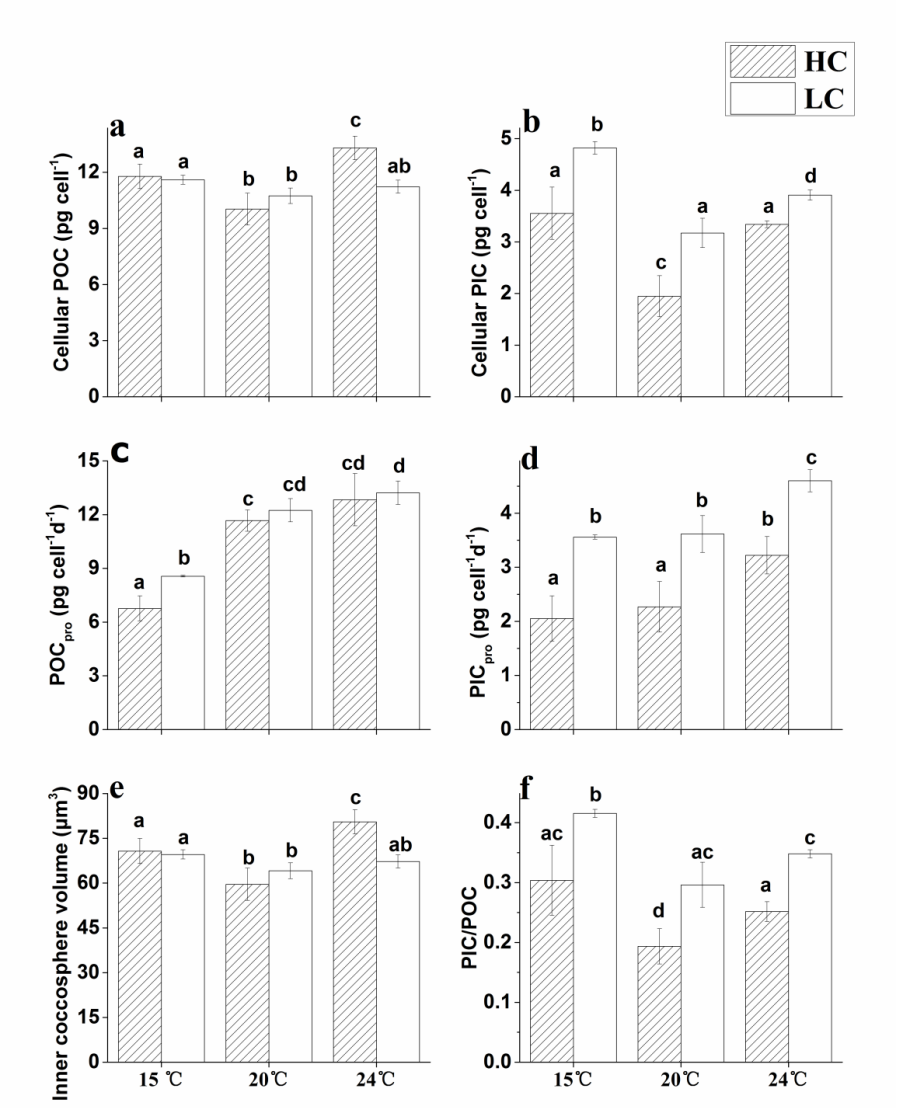

792

793

794

Biogeosciences Discuss., https://doi.org/10.5194/bg-2017-269
Manuscript under review for journal Biogeosciences
Discussion started: 29 June 2017

795 Fig. 4

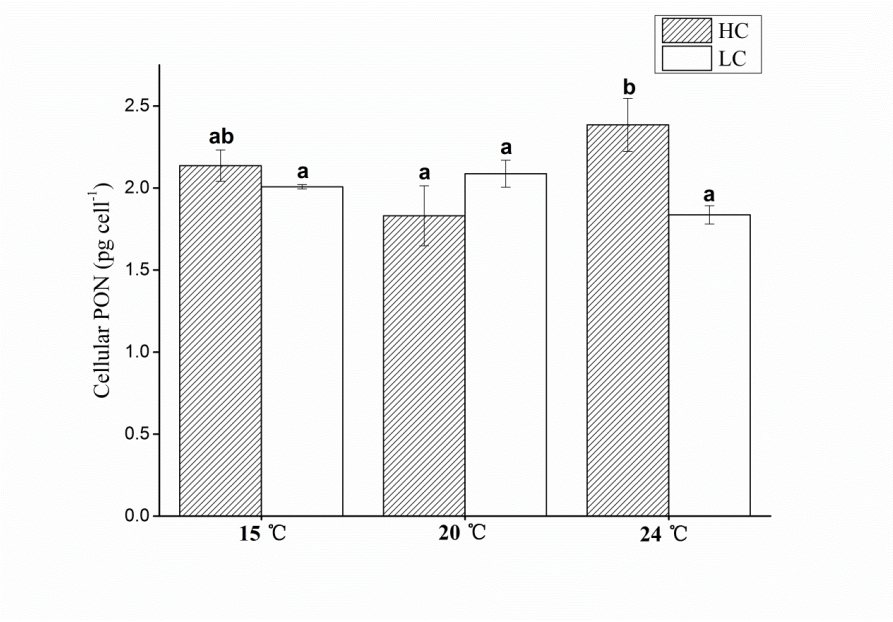

796
797
798
799
800
801
802
803
804
805
806
807
808

Biogeosciences Discuss., https://doi.org/10.5194/bg-2017-269
Manuscript under review for journal Biogeosciences
Discussion started: 29 June 2017

809 Fig. 5

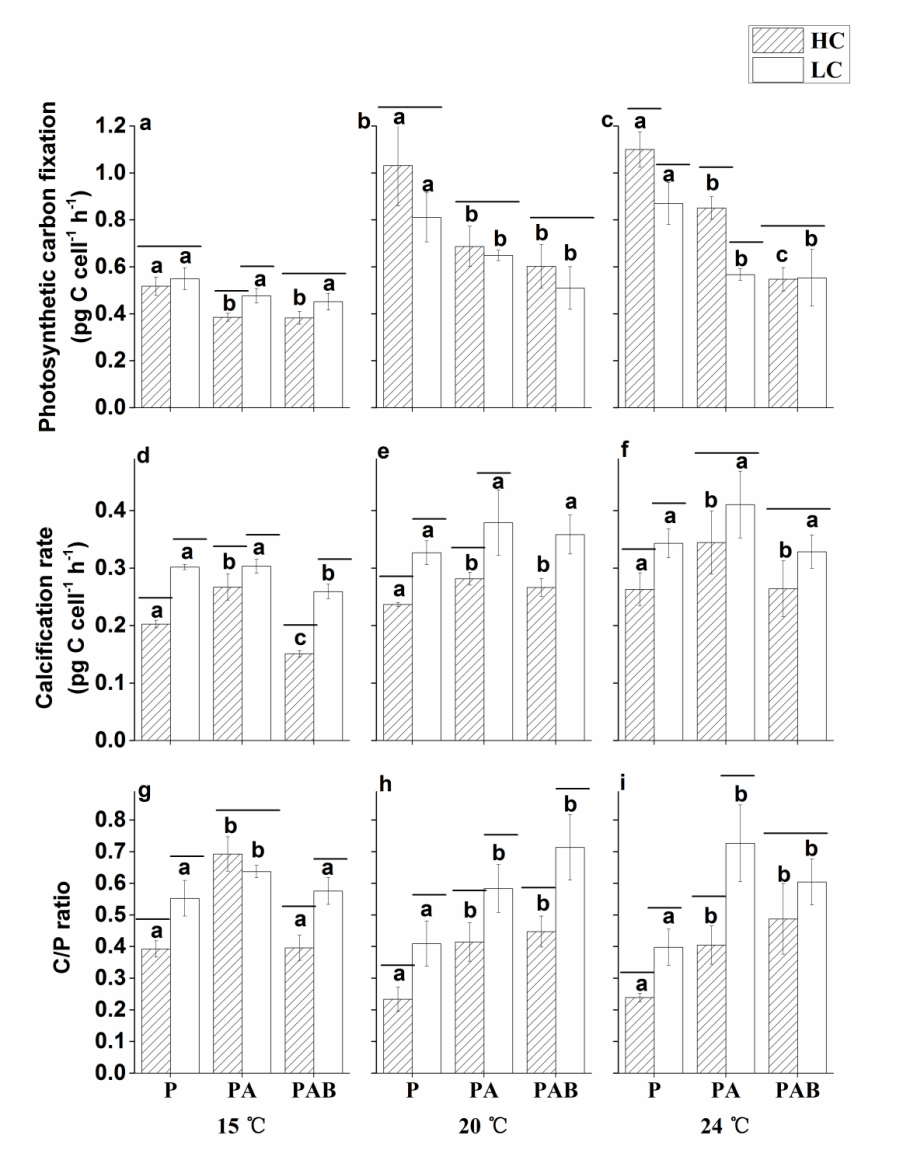

810

811

812

Biogeosciences Discuss., https://doi.org/10.5194/bg-2017-269
Manuscript under review for journal Biogeosciences
Discussion started: 29 June 2017

813 Fig. 6

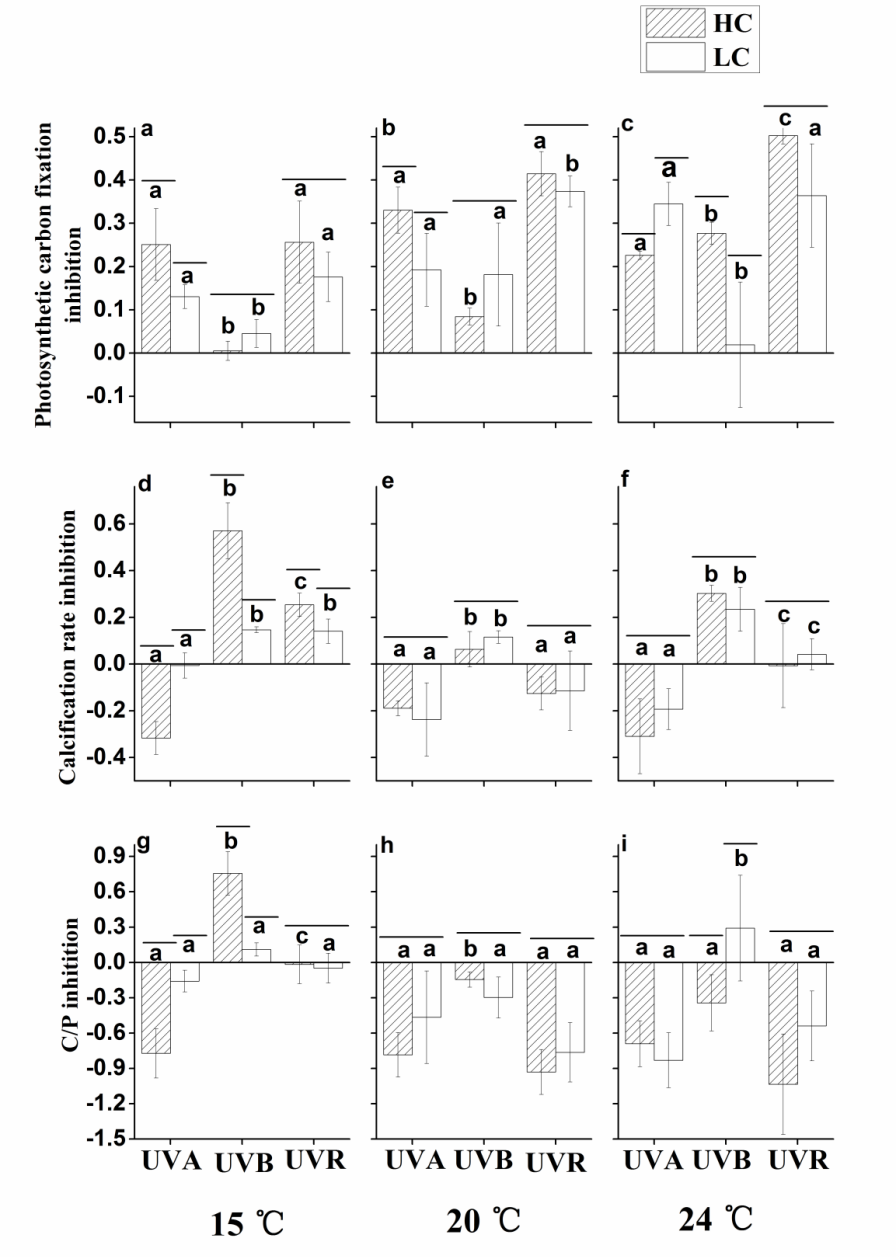

814